

Impact of Laser Treatment on Hydrogenated Amorphous Silicon Properties

Claudia Maurer, Wolfhard Beyer, Markus Hülsbeck, Uwe Breuer, Uwe Rau, and Stefan Haas*

Herein, the application of laser radiation to locally modify the hydrogen distribution within hydrogenated amorphous silicon films on a short time scale is studied. The impact of laser power and irradiation time on the temperature of the silicon layer during the laser treatment and the hydrogen outdiffusion is analyzed. Moreover, the resulting optoelectronic properties of the amorphous silicon are examined. On a timescale of a few seconds or less, the hydrogen concentration in the near-surface region of the silicon layer can be successfully decreased without major impact on the optoelectronic properties.

1. Introduction

Hydrogenated amorphous silicon (a-Si:H) has a long tradition in solar cell and thin film transistor fabrication.^[1–4] For solar cells, intrinsic a-Si:H is used as absorber material in thin film devices and as surface passivation in crystalline wafer-based silicon heterojunction (SHJ) solar cells. In both cases hydrogen is used to passivate dangling bonds, either in the bulk thin film material^[5] or predominantly at the surface of the crystalline wafer.^[6] For both applications, thermal treatments of a-Si:H can play an important role to achieve highly efficient solar cells^[7,8] with a very likely involvement of hydrogen diffusion and redistribution.

The thermal treatment of a-Si:H is usually performed in an oven, where temperature and time are easily adjustable. However, oven annealing is typically a time-consuming process.^[8,9] Furthermore, oven annealing is not energy efficient, because in addition to the annealed thin film, the substrate

and parts of the oven are also heated. Due to these limitations of oven processes, thermal laser annealing is an interesting alternative, which has been used already in the early days of amorphous silicon to modify its properties.^[10] Due to the locally confined absorption of laser radiation in the a-Si:H layer, laser processing can be energy efficient. In addition, the excitation within a small volume in combination with high laser intensities leads to large heating and cooling rates and thus potentially to fast processing. Furthermore, a spatially

resolved treatment is possible.

In this work, we first discuss some results obtained using a continuous wave (CW) laser which clarify the relation^[11] between hydrogen diffusion in bulk material, hydrogen outdiffusion, and the optical photodarkening effect.


We then examine the application of a high-power Q-switched diode pumped solid state slab laser^[12] with a wavelength of 532 nm for thermal laser annealing. This laser is a workhorse for industrial laser material processing. The high laser power enables high area throughput and thus short processing time. We first investigated whether the large area treatment with a pulsed laser leads to similar hydrogen diffusion as a small area treatment with CW laser radiation. In addition, we studied the influence of the laser treatment on characteristic material properties such as photo- and dark conductivity and sub-bandgap absorption. These properties can give information on the concentration of deep defects^[13,14] which may lead to a deterioration of the material quality during laser processing.

2. Experimental Section

In this work, a-Si:H layers with a thickness of ≈ 350 nm were studied, deposited on 10×10 cm² Corning Eagle XG substrates by plasma-enhanced chemical vapor deposition (PECVD) using hydrogen–silane (SiH₄) gas mixtures. For the studies using the CW laser, the substrates were covered with a thin layer of SiO₂. Here, additionally samples with a thickness of ≈ 750 nm were used for selected investigations (cf. Figure 2). The deposition conditions (including a substrate temperature of about 185 °C) were those used for good-quality thin film silicon solar cells.^[15] As measured by infrared absorption, the a-Si:H layers had an initial hydrogen concentration of $c_H = 14$ –15 at%. For the CW laser study, deuteriosilane (SiD₄) was used for the upper 50 nm so that the interdiffusion between the two hydrogen isotopes ¹H (H, hydrogen proper) and ²H (D, deuterium) could be studied.^[11]

Dr. C. Maurer,^[†] Dr. W. Beyer, M. Hülsbeck, Prof. U. Rau, Dr. S. Haas
IEK5 – Photovoltaik
Forschungszentrum Jülich GmbH
Leo-Brandt-Straße, 52425 Jülich, Germany
E-mail: st.haas@fz-juelich.de

Dr. U. Breuer
ZEA3 – Analytik
Forschungszentrum Jülich GmbH
Leo-Brandt-Straße, 52425 Jülich, Germany

 The ORCID identification number(s) for the author(s) of this article can be found under <https://doi.org/10.1002/adem.201901437>.

^[†]Present address: Amphos GmbH, Kaiserstraße 100, 52134 Herzogenrath, Germany

© 2020 The Authors. Published by WILEY-VCH Verlag GmbH & Co. KGaA, Weinheim. This is an open access article under the terms of the Creative Commons Attribution License, which permits use, distribution and reproduction in any medium, provided the original work is properly cited.

DOI: 10.1002/adem.201901437

Laser treatments were performed in ambient atmosphere using laser sources with a wavelength of 532 nm. The conditions used for the CW treatment were reported in Beyer et al.^[11] A circular laser spot with Gaussian intensity profile was used. For the treatment with laser pulses, an Edgewave HD30II-E Innoslab was used. The laser exhibits a pulse duration of 7 ns and was used at a repetition rate of 40 kHz. A cylindrical lens and a rectangular aperture were used to form a rectangular laser beam on the sample, resulting in an irradiated area of $\approx 5 \times 9 \text{ mm}^2$ with a 2D top-hat-like intensity distribution. The irradiation time of the pulsed laser was defined as the time between first laser pulse and last laser pulse of a contiguous pulse sequence. The sample temperature was monitored with a LumaSense IMPAC IN 5/5 plus pyrometer.

The influence of the laser treatment on hydrogen diffusion was studied by secondary ion mass spectrometry (SIMS) measurements,^[11] and on hydrogen concentration by both SIMS and Raman spectroscopy in backscattering mode.^[16] Here, a Raman excitation wavelength of $\lambda = 532 \text{ nm}$ was used, which led to a Raman information depth of $\approx 50 \text{ nm}$ ^[16] due to the Beer–Lambert law. Photo- and dark conductivity measurements were performed under vacuum conditions on films equipped with coplanar electrodes after laser treatment. For photoconductivity an illumination with 100 mW cm^{-2} (near AM 1.5) was used. The sub-bandgap absorption was measured by photo-thermal deflection spectroscopy according to Jackson et al.^[17]

3. Results and Discussion

3.1. Continuous Wave Laser Treatment

Depending on laser scan speed v , which defines a laser residence time t^* ($t^* = S/v$ with S the laser spot diameter) the a-Si:H films heat up and hydrogen diffuses as the hydrogen diffusion in a-Si:H is known to follow Arrhenius dependences.^[11] The hydrogen outdiffusion is visible by the photodarkening effect,^[10,11] which is clearly shown in **Figure 1a** by the darker color of the a-Si:H film scanned at a speed of $v = 2 \text{ mm s}^{-1}$, as compared to the others. For this sample the SIMS depth profile of hydrogen shown in **Figure 1b** shows a strong reduction in hydrogen concentration toward the surface and the film substrate interface. For the film scanned with $v = 10 \text{ mm s}^{-1}$ basically no photodarkening (see **Figure 1a**), and an almost constant hydrogen concentration in depth is observed. The temperature in the laser spot can be calculated from the treatment conditions.^[11] For the scan speed of 2 mm s^{-1} ($t^* = 0.35 \text{ s}$) a temperature of $T \approx 780^\circ\text{C}$ is determined, while for the scan speed of 10 mm s^{-1} ($t^* = 0.07 \text{ s}$) a temperature of $T \approx 500^\circ\text{C}$ is obtained. Note that the spike in hydrogen concentration at a (relative) sputter time of $t = 0.25$ marks the interface between the hydrogenated and the deuterated material. This interface, not being perfect, tends to involve voids or bubbles covered with surface-bound hydrogen upon annealing, i.e., leads to some local hydrogen accumulation. Also note that the decrease of the hydrogen concentration toward the substrate in the annealed state, i.e., outdiffusion of hydrogen near the film–substrate interface, is not always observed. Such an outdiffusion of hydrogen requires either a substrate permeable for diffusing

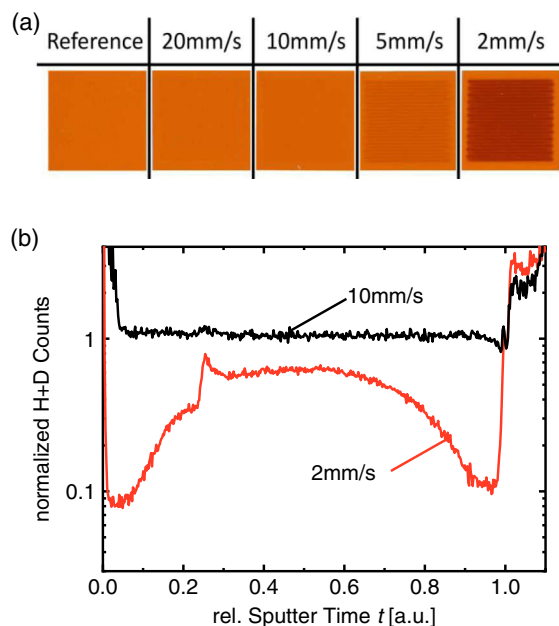


Figure 1. a) Transmitted light image of a-Si:H treated by scanning with a CW laser at 2.7 W laser power (from the a-Si:H layer side) with various laser scan speeds v (reprinted from Beyer et al.,^[11] with the permission of AIP Publishing). b) SIMS depth profiles of hydrogen (H + D), normalized to ^{30}Si signal for the a-Si:H films of **Figure 1a**, treated with laser scan speeds of 2 and 10 mm s^{-1} for illumination from layer side.

H_2 or a poor substrate–film interface with a high concentration of voids. The present films were deposited on SiO_2 -coated Corning substrates where the intention of the SiO_2 layer is to provide a medium for H_2 outdiffusion.^[18]

As discussed in Beyer et al.,^[11] measurements of D–H interdiffusion allow the evaluation of both the hydrogen diffusion length L and the temperature T in the laser spot. In **Figure 2a** it is demonstrated that for a fixed intentional photodarkening^[11] the measured hydrogen diffusion length L is constant, meaning that hydrogen diffusion can directly determine optical properties of a-Si:H. This happens when hydrogen outdiffusion leads to a reduction of the bandgap.^[10,11] **Figure 2b** shows the temperatures T reached in the laser spot as a function of laser power P (applied from the glass side of the film) and laser scan speed v . The results agree with an expected linear dependence of temperature on laser power.^[19] Smaller scan speeds v and thus longer laser residence time t^* tend to increase the obtained temperature T .

3.2. Pulsed Laser Treatment

Figure 3 shows the increase and decrease of the measured time-dependent layer temperature for an irradiation time of $t_{\text{on}} = 3 \text{ s}$. The average laser power was varied from $P_{\text{avg}} = 11.7 \text{ W}$ (black line) to $P_{\text{avg}} = 24.9 \text{ W}$ (magenta line). Similar results were obtained with an irradiation time of 4, 7, and 10 s (not shown here). A rather strong increase in temperature over the entire irradiation time was observed for all applied irradiation time periods. The black arrow marks the time when the laser is switched off. Note that for the conditions used, the temperature does not reach a steady-state value over the duration of the laser irradiation.

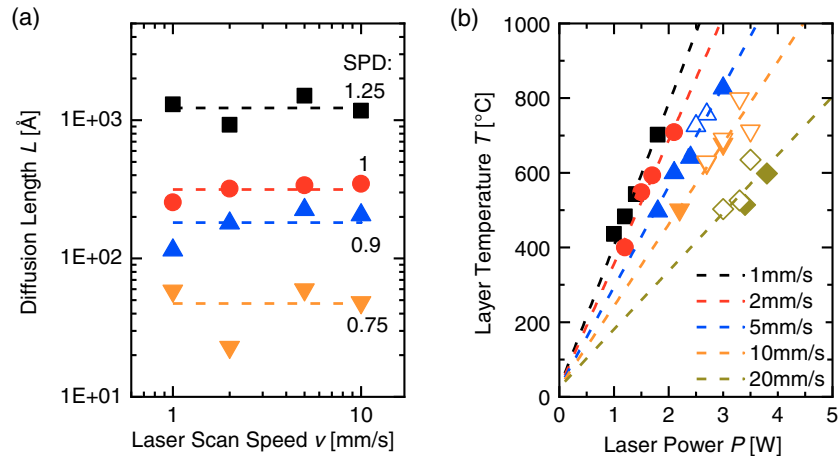


Figure 2. a) Hydrogen diffusion length L (in the bulk) as a function of laser scan speed v for various intentional photodarkening levels, measured in multiples of a standard photodarkening level termed SPD.^[11] Film thickness here was 750 nm. b) Layer temperature T in the laser spot as a function of laser power P for various scan speeds v . Laser illumination here was from glass side. Closed symbols refer to an a-Si thickness of 750 nm, open symbols to an a-Si thickness of 350 nm. Reprinted from Beyer et al.,^[11] with the permission of AIP Publishing.

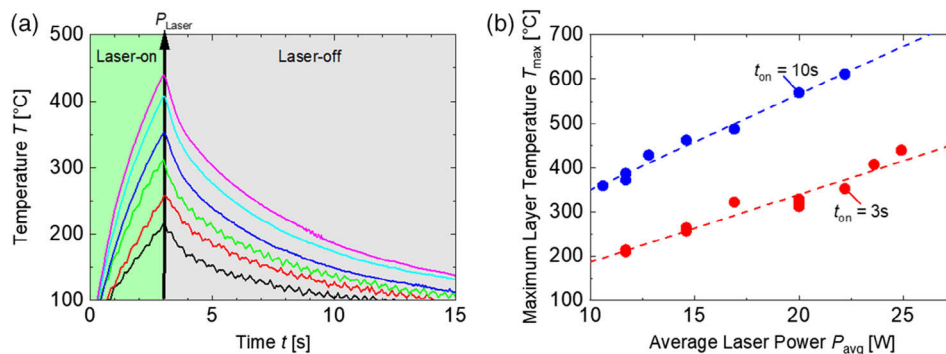


Figure 3. a) Time-dependent layer temperature for the laser treatment time of $t_{on} = 3$ s. The average laser power was increased from $P_{avg} = 11.7$ W (black curve) to $P_{avg} = 24.9$ W (magenta curve). The black arrow marks the time when the laser is switched off. The increased noise level for low laser powers is due to an inappropriate setting of the sampling rate of the pyrometer for the respective measurements. b) Maximum layer temperature depending on the laser power for an irradiation time t_{on} of 3 s (red dots) and 10 s (blue dots). The dashed lines refer to linear fits for the measured values.

In Figure 3b the maximum layer temperature is plotted as a function of the applied laser power for irradiation time periods t_{on} of 3 and 10 s. The graphs show that a linear dependence of the maximum layer temperature is present for a wide range of the applied laser power.

The shape of the temperature evolution in Figure 3a follows generally the behavior expected when using a 1D transient model and a flat, surface-heated semi-infinite body for the calculation of the heat distribution.^[20] Here, the heat distribution can be calculated analytically and a square root time dependence is determined for the surface temperature. The analytical model also predicts the observed, almost linear dependence of the maximum layer temperature on the applied laser power. This linear dependence is also in agreement with the results found for the CW laser treatment (cf. Figure 1b).

The Raman-detected relative hydrogen concentration is shown in Figure 4 as a function of maximum layer temperature T_{max} . The black symbols ("ref") refer to as-deposited samples.

The scatter in the data shows the fluctuation of the hydrogen concentration between different samples and sample positions. The color of the other symbols indicates the irradiation time (red 3 s, magenta 4 s, green 7 s, blue 10 s). The data show that the hydrogen concentration primarily depends on the maximum process temperature T_{max} and not so much on the irradiation time t_{on} . This agrees with the theory of diffusion where the diffusion length L has a square root dependence on time but an exponential dependence on temperature.^[11] Therefore, T_{max} can be used as a reference value to characterize the individually treated samples. As guide to the eye, we additionally plot a locally weighted second-order polynomial regression (loess) curve of all data points.^[21]

Figure 4 shows that the hydrogen concentration steadily decreases with increasing T_{max} . For temperatures above $T_{max} = 600$ °C, the hydrogen concentration is below the detection limit of the Raman spectroscopy system used in this work. Despite the scatter of the data, the results suggest a slight

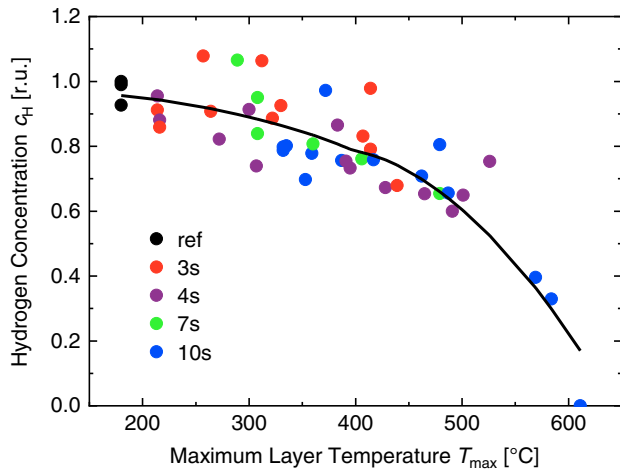


Figure 4. Relative change of the hydrogen concentration c_H detected by Raman as a function of the maximum layer temperature T_{\max} . The as-deposited references are marked by black symbols. The colors refer to the exposure time (red 3 s, magenta 4 s, green 7 s, blue 10 s). As guide to the eye, a loess curve of all data points is also shown.

decrease of c_H already for maximum temperatures below $T_{\max} = 300^\circ\text{C}$, although from hydrogen diffusion and effusion measurements little hydrogen mobility is expected for this type of a-Si:H at temperatures $< 300^\circ\text{C}$.^[22]

Aiming for a better understanding of the dependence of Raman-detected hydrogen concentration as a function of T_{\max} , the hydrogen diffusion process induced by the laser treatment was modeled by means of 1D finite element (FEM) simulations. The time-dependent advection–diffusion solver of the FEM tool ELMER^[23] was used. The surface of the sample as well as the substrate was defined as a hydrogen sink, as this behavior was found by the SIMS measurements of CW laser hydrogen diffusion in a-Si:H (see Figure 2). Selected temperature versus time profiles measured during the laser treatment (cf. Figure 3a)

were taken as input parameter. A diffusion coefficient prefactor of $D_0 = 10^{-7} \text{ m}^2 \text{ s}^{-1}$ and an activation energy of $E_A = 1.3 \text{ eV}$ were used.^[22] We note that using a single Arrhenius dependence of the hydrogen diffusion coefficient for the whole hydrogen effusion process is a very strong simplification.^[13,22] The simulations were conducted for four processes with an irradiation time of $t_{\text{on}} = 3 \text{ s}$ and three processes with an irradiation time of $t_{\text{on}} = 10 \text{ s}$.

Figure 5a shows the simulated hydrogen concentration profiles $c'_{H,\text{SIM}}$ within the amorphous silicon layer as a function of the maximum layer temperature T_{\max} . As expected, the hydrogen profiles indicate a depletion of hydrogen near the film surface and the film–substrate interface. This depletion is a result of the hydrogen outdiffusion with increasing temperature T_{\max} . The similarity to Figure 2b is apparent. Up to a maximum layer temperature T_{\max} of about 350°C (3 s) little changes of the assumed rectangular original hydrogen concentration profile occur. We note that a similar sine-function dependence of hydrogen concentration on depth for high annealing temperatures was obtained when the diffusion equation was solved to explain the temperature dependence of hydrogen effusion.^[24] Figure 5b shows a comparison between the hydrogen concentration $c_{H,\text{SIM}}$ calculated from the simulated hydrogen depth profiles $c'_{H,\text{SIM}}$ and the hydrogen content c_H taken from the loess curve of the Raman measurements. The hydrogen concentration $c_{H,\text{SIM}}$ was calculated using the hydrogen concentration profiles from Figure 5a, taking into account the limited Raman information depth. The comparison shows that the simulated hydrogen profiles represent the trend detected by the Raman hydrogen concentration measurements. Nevertheless, it is important to note that for temperatures up to 480°C (blue), most of the hydrogen in the layer is not affected by the laser treatment (Figure 5a). However, the measured hydrogen concentration by Raman c_H (Figure 4) already shows some decrease of the concentration. This may be because Raman measures only a thin surface layer. Other reasons could be 1) that only a single Arrhenius dependence of hydrogen diffusion was used for the

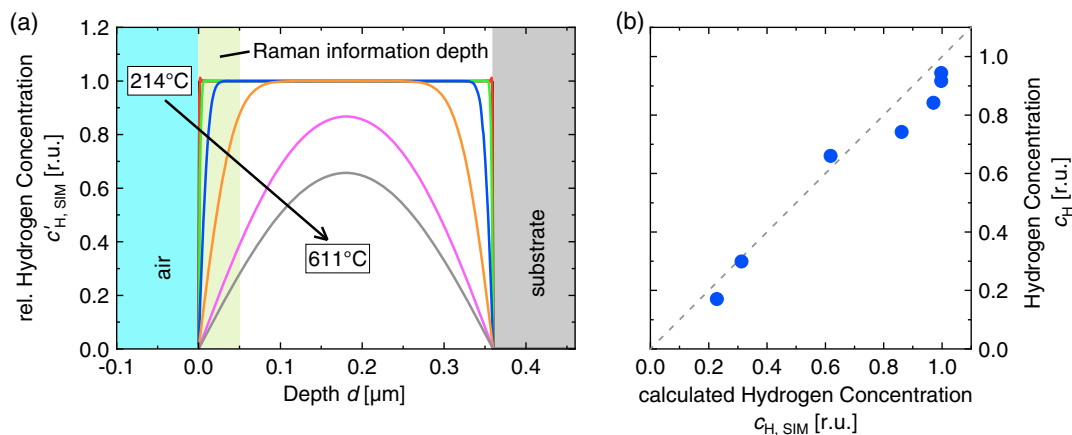


Figure 5. a) Simulated hydrogen concentration profiles $c'_{H,\text{SIM}}$ for different maximum layer temperatures T_{\max} (black 214°C and 3 s, red 264°C and 3 s, green 353°C and 3 s, blue 439°C and 3 s, orange 479°C and 10 s, magenta 584°C and 10 s, grey 611°C and 10 s). In addition, the range of the Raman information depth is marked in light green. Note that hydrogen concentration profiles $c'_{H,\text{SIM}}$ for maximum layer temperatures T_{\max} of 214, 264, and 353°C are almost on top of each other and thus difficult to distinguish. b) Comparison between the hydrogen content $c_{H,\text{SIM}}$ calculated from the simulated hydrogen depth profiles $c'_{H,\text{SIM}}$ and the hydrogen content taken from the Raman loess curve c_H .

simulation while it is known that hydrogen diffusion in a-Si:H depends on the hydrogen concentration and 2) that near the film surface not only hydrogen diffusion but also hydrogen surface desorption processes may play a role.^[13,22]

To gain some insight into the influence of the laser treatment on deep defects, the sub-bandgap absorption^[14] as well as photo- and dark conductivities were measured.^[13,25] Samples with $264^{\circ}\text{C} \leq T_{\text{max}} \leq 655^{\circ}\text{C}$ were used. The influence of the laser treatment on the absorption coefficient α (versus photon energy E_{ph}) of a-Si:H is shown in Figure 6. For measured maximum process temperatures up to $T_{\text{max}} = 584^{\circ}\text{C}$ no influence on the sub-bandgap absorption at a photon energy of $E_{\text{ph}} = 1.2\text{ eV}$ is observed. An increase of the sub-bandgap absorption is found exclusively at $T_{\text{max}} > 600^{\circ}\text{C}$. Here, the sub-bandgap absorption (at 1.2 eV) increases over one order of magnitude for $T_{\text{max}} = 655^{\circ}\text{C}$ as compared to the untreated reference. In addition to the increase in sub-bandgap absorption, Figure 6 also shows a shift of the E_{04} optical gap to lower energies with decreasing hydrogen content at $T_{\text{max}} > 400^{\circ}\text{C}$. This is in agreement with the observed photodarkening of the CW laser-treated samples (see Figure 2).

The influence of the maximum temperature T_{max} during laser treatment on the photo- and dark conductivity is shown in Figure 7. For comparison, the sub-bandgap absorption $\alpha_{1.2\text{ eV}}$ at a photon energy of $E_{\text{ph}} = 1.2\text{ eV}$ and the optical gap E_{04} are also plotted. The photoconductivity σ_{ph} (Figure 7, red stars) is in the same order of magnitude for all analyzed samples. However, a strong increase of σ_{d} is observed for maximum process temperatures $T_{\text{max}} \geq 600^{\circ}\text{C}$ (Figure 7, black squares). For these samples, σ_{d} increases over four orders of magnitude compared to the as-deposited reference. In the same temperature range where the dark conductivity σ_{d} increases the sub-bandgap absorption $\alpha_{1.2\text{ eV}}$ increases, too.

These latter results are consistent with the measured and calculated (Figure 5a) hydrogen concentration values, which indicate values less than 1–2 at% at $T_{\text{max}} > 600^{\circ}\text{C}$ in the

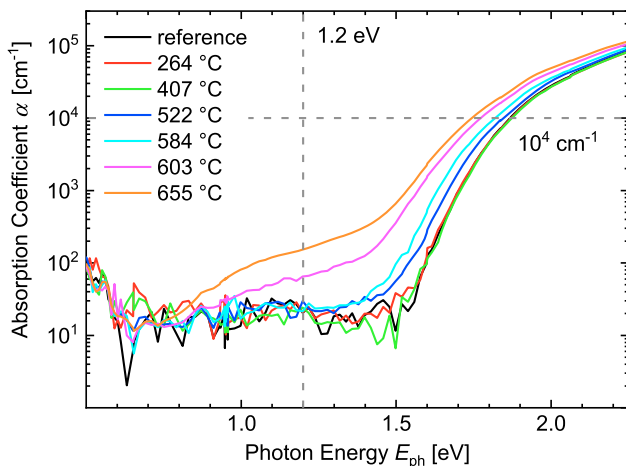


Figure 6. Influence of the laser treatment of a-Si:H on the sub-bandgap absorption. The sub-bandgap absorption is shown for maximum process temperatures $264^{\circ}\text{C} \leq T_{\text{max}} \leq 655^{\circ}\text{C}$. The vertical dashed line indicates the sub-bandgap absorption at 1.2 eV , while the horizontal dashed line marks the E_{04} optical gap.

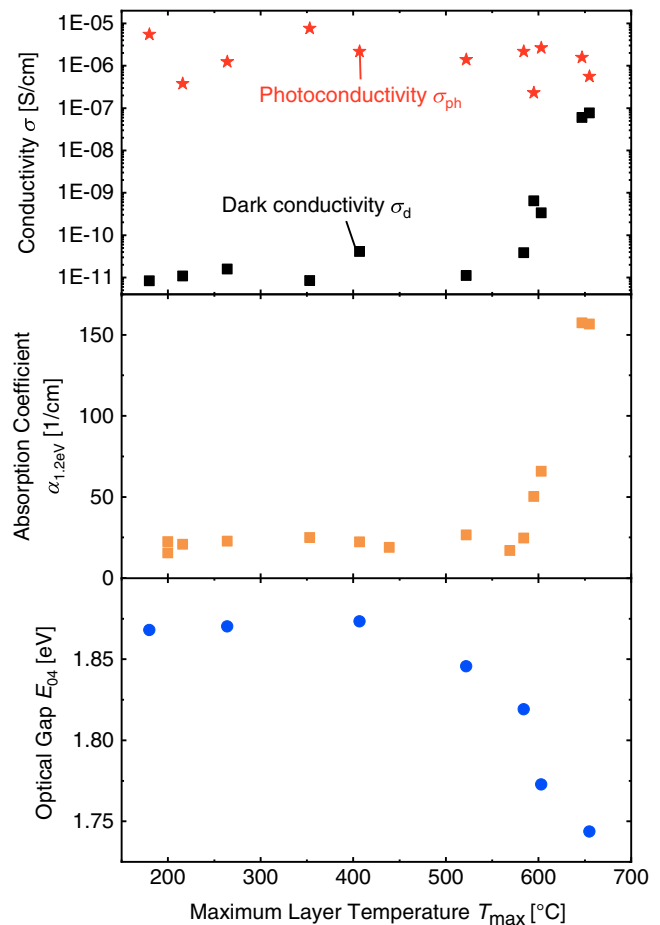


Figure 7. Influence of the maximum process temperature T_{max} on (top) dark conductivity σ_{d} (black squares) and photoconductivity σ_{ph} (red stars), sub-bandgap absorption coefficient $\alpha_{1.2\text{ eV}}$ (middle), and optical gap E_{04} (bottom).

near-surface region. For such a material, electrical conductivity is known to proceed by hopping conduction via defect states near midgap,^[13,26] e.g., dangling bonds, and dark conductivity values of 10^{-6} S cm^{-1} were reported at room temperature. This is consistent with the dark conductivity σ_{d} of 10^{-7} S cm^{-1} reported here (Figure 7) considering the fraction of $\approx 10\%$ of the layer thickness (see Figure 5a) affected by hydrogen outdiffusion. This near-surface layer with enhanced defect concentration is not expected to change the photoconductivity σ_{ph} greatly as long as the affected layer volume (thickness) does not involve a major part of the film, as the photoconductivity is also measured in coplanar configuration. The change in the optical gap E_{04} with rising maximum temperature T_{max} differs from the changes in dark conductivity σ_{d} and the sub-bandgap absorption $\alpha_{1.2\text{ eV}}$ because it starts at lower temperatures T_{max} near 400°C . These changes are not caused by the increase in density of localized states but by the reduction in hydrogen concentration.^[13] Directly related to this reduction of the optical bandgap is the photodarkening effect.

The present results demonstrate that the laser-induced temperature rise influences optoelectronic properties of a-Si:H primarily via hydrogen outdiffusion. In the depth range where

hydrogen diffuses out, the optical gap shrinks. In this region, even a high concentration of defects with states near midgap can form. The impact on the electronic properties depends thus on the thickness of the a-Si:H films. Thinner films are more strongly affected than thicker ones. By a proper choice of laser parameters, a tailored manipulation of film properties appears possible. It is therefore also possible to generate specific flows of hydrogen out of a layer. For the investigated material, the data of Figure 4 and 7 show in particular that for laser annealing at a maximum layer temperature of $\approx 500^\circ\text{C}$ almost half of the Raman-measured hydrogen is driven out, whereas the photo- and dark conductivities as well as the sub-bandgap absorption remain unchanged.

4. Conclusions

We demonstrated that by using CW as well as pulsed laser sources at a wavelength of $\lambda = 532\text{ nm}$ the hydrogen concentration of a-Si:H films on glass can be reduced greatly in the surface and (depending on the film–substrate interface) in the near-film–substrate interface region. With both laser treatment setups applied, temperatures exceeding 600°C causing significant hydrogen outdiffusion can be obtained in a few seconds or less. In fact, the hydrogen concentration in the near-surface region could be reduced below the detection limit of hydrogen by Raman spectroscopy. Whereas a reduction of near-surface and near-interface hydrogen concentration to 1–2 at% leads to rather significant electrooptical changes, a reduction of the surface hydrogen by almost a factor of 2 has little negative impact on either the electrical or optical properties of a-Si:H. Using laser-induced dehydrogenization, it is possible to modify an amorphous silicon layer over a wide parameter range without strong impact on the electrical properties. The influence of the intense irradiation on the distribution of hydrogen is supported by finite element simulations.

Acknowledgements

The authors would like to thank A. Lambertz, T. Merdzhanova, and D. Weigand for sample preparation, the group of G. Andr  at Leibniz-Institut f r Photonische Technologien in Jena, Germany, for the CW laser scanning, S. Moll, J. Klomfa , and O. Thimm for the conductivity and PDS measurements, as well as the company EdgeWave in W rselen, Germany, for supplying the high-power slab laser. Part of the work was financed by BMU (project numbers 0325446A and B).

Conflict of Interest

The authors declare no conflict of interest.

Keywords

amorphous silicon, hydrogen diffusion, laser treatment

Received: November 22, 2019

Revised: February 7, 2020

Published online: March 3, 2020

- [1] D. E. Carlson, C. R. Wronski, *Appl. Phys. Lett.* **1976**, 28, 671.
- [2] Y. Hamakawa, K. Fujimoto, K. Okuda, Y. Kashima, S. Nonomura, H. Okamoto, *Appl. Phys. Lett.* **1983**, 43, 644.
- [3] M. Tanaka, M. Taguchi, T. Matsuyama, T. Sawada, S. Tsuda, S. Nakano, H. Hanafusa, Y. Kuwano, *Jpn. J. Appl. Phys.* **1992**, 31, 3518.
- [4] *Thin Film Transistors* (Ed: Y. Kuo), Springer US, Boston, MA **2004**.
- [5] Z. E. Smith, S. Wagner, *Phys. Rev. B* **1985**, 32, 5510.
- [6] J. I. Pankove, M. L. Tarng, *Appl. Phys. Lett.* **1979**, 34, 156.
- [7] D. L. Staebler, C. R. Wronski, *Appl. Phys. Lett.* **1977**, 31, 292.
- [8] S. De Wolf, A. Descoeurdes, Z. C. Holman, C. Ballif, *Green* **2012**, 2, 7.
- [9] K. Wilken, F. Finger, V. Smirnov, *Energy Proc.* **2015**, 84, 17.
- [10] D. L. Staebler, *J. Appl. Phys.* **1979**, 50, 3648.
- [11] W. Beyer, G. Andr , J. Bergmann, U. Breuer, F. Finger, A. Gawlik, S. Haas, A. Lambertz, F. C. Maier, N. H. Nickel, U. Zastrow, *J. Appl. Phys.* **2018**, 124, 153103.
- [12] K. Du, *Laser Tech. J.* **2010**, 7, 39.
- [13] W. Beyer, *Tetrahedrally-Bonded Amorphous Semiconductors*, Springer US, Boston, MA **1985**, pp. 129–146.
- [14] N. Wyrsh, F. Finger, T. J. McMahon, M. Vanecek, *J. Non. Cryst. Solids* **1991**, 137–138, 347.
- [15] A. Lambertz, F. Finger, R. E. I. Schropp, U. Rau, V. Smirnov, *Prog. Photovoltaics Res. Appl.* **2015**, 23, 939.
- [16] C. Maurer, S. Haas, W. Beyer, F. C. Maier, U. Zastrow, M. H lsbeck, U. Breuer, U. Rau, *Thin Solid Films* **2018**, 653, 223.
- [17] W. B. Jackson, N. M. Amer, A. C. Boccara, D. Fournier, *Appl. Opt.* **1981**, 20, 1333.
- [18] W. Beyer, F. Einsele, *Advanced Characterization Techniques for Thin Film Solar Cells* (Eds: D. Abou-Ras, T. Kirchartz, U. Rau), Wiley-VCH Verlag GmbH & Co. KGaA, Weinheim, Germany **2016**, p. 569.
- [19] M. Lax, *J. Appl. Phys.* **1977**, 48, 3919.
- [20] J. Mazumder, *JOM* **1983**, 35, 18.
- [21] W. S. Cleveland, S. J. Devlin, *J. Am. Stat. Assoc.* **1988**, 83, 596.
- [22] W. Beyer, *Sol. Energy Mater. Sol. Cells* **2003**, 78, 235.
- [23] I. Kondov, G. Sutmann, *Multiscale Modelling Methods for Applications in Materials Science Lecture Notes*, Forschungszentrum J lich GmbH, J lich, Germany **2013**.
- [24] W. Beyer, H. Wagner, *J. Appl. Phys.* **1982**, 53, 8745.
- [25] M. Stutzmann, M. C. Rossi, M. S. Brandt, *Phys. Rev. B* **1994**, 50, 11592.
- [26] I. P. Zvyagin, I. A. Kurova, N. N. Ormont, *Phys. Status Solidi C* **2004**, 1, 101.